AAS 23-282

DOUBLE LUNAR SWINGBY TRAJECTORIES TO NEAR-GEOSTATIONARY ORBIT

Stephen West,[1] John Carrico,[2] and Mike Loucks[3]

Lunar gravity assists can be used to reduce inclination and raise perigee radius to transfer a spacecraft from lunar rideshare launch to near-geostationary orbit. Double lunar swingby orbits relax the targeting constraints on the first lunar swingby and increase compatibility with lunar rideshare opportunities. Both short- and long-period solutions exist, offering a trade-off between time-of-flight and maximum spacecraft-to-Earth range. The short-period orbits have the added complexity of a perigee maneuver below GEO and within the Outer Van Allen Belts. Time-of-flight from injection to first near-geostationary perigee ranges from ~40 days (short-period) to ~75-105 days (long-period). These transfers require ~1,000-1,100 m/s for orbit lowering and an additional 20-90 m/s for cislunar maneuvering.

INTRODUCTION

Interest in civil, defense, and commercial missions in the region of space beyond geostationary orbit (GEO) has increased dramatically in recent years. Frequent launches to high-energy orbits offer opportunities for small spacecraft rideshare to cislunar or lunar orbit. One potential application of these lunar rideshare launches is spacecraft bound for GEO by way of a lunar swingby. With the increasing scarcity of geostationary transfer orbit (GTO) or direct to GEO launches, lunar rideshares may become a more accessible option.

A lunar rideshare launch typically injects the spacecraft into an orbit with an inclination of approximately 28.5° and apogee near lunar orbit radius. To return to near-GEO, a spacecraft must simultaneously reduce inclination and raise perigee. Given the lunar encounter targeted by the rideshare launch, the spacecraft can use lunar gravity assists (LGrAs) to target the desired operational orbit. The range of possible gravity assist geometries is determined by the launch conditions. As a secondary payload, the spacecraft must be able to accommodate variations in the rideshare launch targets as they evolve for the primary mission. Space Exploration Engineering (SEE) has developed a range of mission trajectories robust to variations in the lunar launch targets.

To accomplish the return to GEO with a single gravity assist, the lunar encounter must occur within a few degrees of the Earth's equatorial plane such that the post-swing-by orbit has inclination near 0°. Since the rideshare launch is delivering a lunar lander as the primary payload, the initial lunar encounter, even if targeted near the Earth's equatorial plane, does not result in a suitable post-

[1] Sr. Flight Dynamics Engineer, Space Exploration Engineering, LLC, 324 Main St. Laurel, MD
[2] Owner and CTO, Space Exploration Engineering, LLC, 324 Main St. Laurel, MD
[3] Owner and CEO, Space Exploration Engineering, LLC, 324 Main St. Laurel, MD

swing-by transfer orbit. As such, after separation from the upper-stage of the launch vehicle, the spacecraft performs a mid-course correction (MCC) maneuver to retarget the lunar encounter to achieve the desired post-swing-by transfer orbit. Policastri et al previously described a set of reference trajectories employing a single swing-by for representative launches targeting the lunar encounter near the Earth's equatorial plane[1].

Constraints imposed by the primary lunar lander payload (e.g. time-of-flight, lighting conditions at the intended landing site) may require that the launch target a lunar encounter significantly above or below the Earth's equatorial plane. In this case, the MCC required to target the equatorial lunar swing-by becomes infeasibly large (100s m/s). As an alternative, the spacecraft can perform multiple lunar gravity assists to setup the required lunar encounter geometry and achieve the desired final transfer orbit. Since the first swingby only needs to target the appropriate geometry at the second swingby, the required deviation from the initial post-launch trajectory is small and the MCC magnitude remains feasible (10s m/s). Given a set of representative lunar rideshare launches in April and May 2024 (that do not target the lunar encounter near the equatorial plane), SEE developed double lunar swingby trajectories that return the spacecraft to GEO graveyard orbit.

BACKGROUND

The concept of using a lunar swing-by to return a spacecraft to Earth was the foundation for the Apollo program's free-return trajectories[2]. The analysis approach described by Battin and Miller generates two Earth-centered two-body orbits that contain the launch and desired landing site, respectively. These two-body orbits are iteratively adjusted until the Moon-centered trajectory through the lunar sphere of influence is continuous.

Sun synchronous double lunar swingby orbits have enabled missions studying Earth's geomagnetic tail. In this application, a pair of lunar gravity assists is selected with multiple revolutions in a smaller transfer orbit connecting the two lunar encounters. Dunham and Davis[3] catalog 43 of these orbits with a wide range of orbit periods. They describe a method of computing double lunar swingby orbits in a simplified dynamical model using a combination of a broad search algorithm to identify potential solutions and a Newton-Rhapson iterator to generate continuous solutions from an initial guess. Carrico et al[4] describe a method for generating similar orbits that uses sequential single-shooting differential correctors to converge a solution in a full-force model. This method was employed for both the WIND and Geotail missions.

Double lunar swingby orbits have also enabled "rescue" of satellites stranded in their initial geostationary transfer orbit (GTO). The AsiaSat-3 satellite performed the first commercial lunar swingby while flying this type of trajectory after a launch failure left it in GTO with an unusable inclination of 51.6°. By first raising its apogee to near lunar orbit radius, AsiaSat-3 (then renamed HGS-1) was able to perform two lunar gravity assists to reduce inclination and raise perigee[5]. Further orbit lowering captured the satellite into its intended geostationary orbit.

This type of rescue trajectory was studied but not implemented for other stranded GEO satellites including AMC-14 and Arabsat 20. Figure 1 shows a potential trajectory for the AMC-14 recovery developed by Carrico and Loucks.

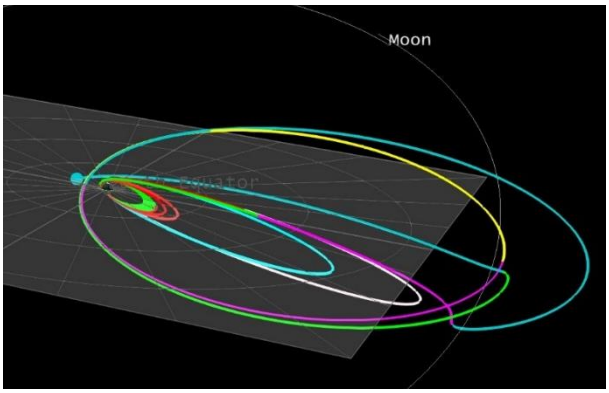

Figure 1. AMC-14 rescue trajectory in the Earth Inertial frame

After the first lunar encounter, AMC-14 would have performed two perigee maneuvers and an apogee maneuver to target the second gravity assist. Figure 2 shows AMC-14's altitude (above a mean spherical Earth) from initial orbit raising to the first GEO-altitude perigee. The black dashed line corresponds to GEO altitude and the gray dotted line is approximately lunar orbit distance.

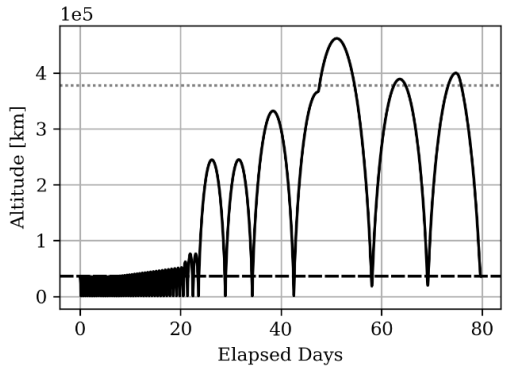

Figure 2. AMC-14 altitude from orbit raising to GEO-altitude

Figure 3 shows the AMC-14 recovery trajectory in three reference frames. From the Earth-Moon rotating pulsating frame (center panel), the two lunar gravity assists are readily apparent.

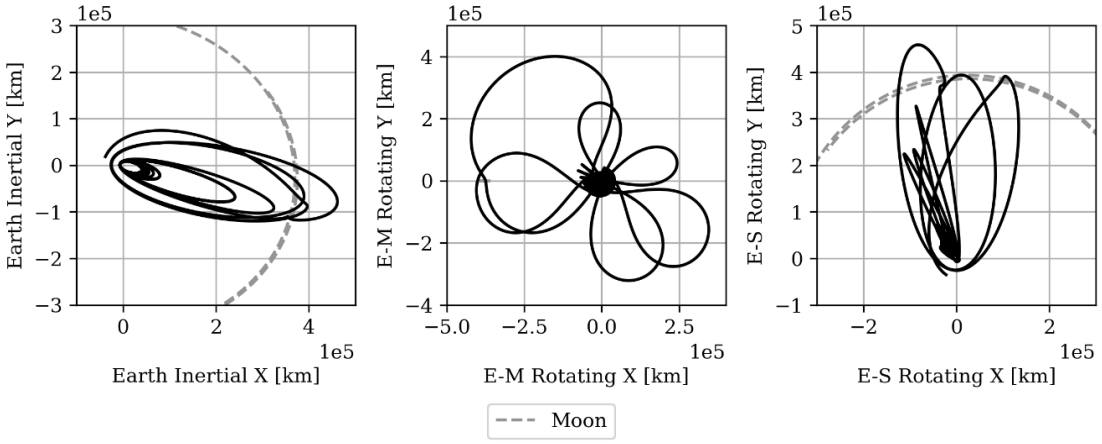

Figure 3. AMC-14 recovery trajectory shown in Earth inertial (left), Earth-Moon rotating pulsating (center), and Earth-Sun rotating pulsating (right) frames

MISSION REQUIREMENTS AND CONSTRAINTS

As a secondary payload launching with a commercial lunar lander, the spacecraft cannot impose requirements on the launch targets. This work uses a set of representative injection states for the April and May 2024 launch periods. These states target a lunar encounter that enables the primary lander payload to capture into orbit and target its landing site. Unlike the GEO rescue double lunar swingby orbits, the lunar rideshare spacecraft does not need further orbit raising after separation. The MCC maneuver diverts the spacecraft from the injection state to its desired trajectory.

To ensure safe disposal, the final lunar swingby targets the GEO graveyard as its destination. Table 1 summarizes the GEO graveyard definition used for this analysis. The perigee radius and eccentricity are selected to be consistent with the Inter-Agency Space Debris Coordination Committee Space Debris Guidelines.[6] No RAAN is specified to avoid an over-constrained targeting problem. Additionally, since the GEO graveyard orbit is above GEO, the spacecraft will drift in the negative in-track direction relative to GEO. If the ultimate destination is a specific GEO slot, the spacecraft can passively drift to this location before inserting into a final location with (comparably) small maneuvers.

Table 1. GEO graveyard orbit requirements

Orbital Elements		Value	Tolerance
Perigee Radius	r_p	42,464 km	±10 km
Eccentricity	e	0	0.003
Inclination	i	0°	±1°
RAAN	Ω	Unconstrained	N/A

SEE developed double lunar swingby orbits that meet these orbit requirements. All trajectories are integrated in AGI's Systems Tool Kit (STK) using a full force model with Earth 21x21 gravity, a point-mass Moon, and representative solar radiation pressure. For trajectory design, STK's Astrogator module[7] supports multiple differential corrector profiles and a robust system for computing orbit parameters and geometry. The following sections present these reference trajectories and summarize key results for launch periods in April and May 2024.

SHORT-PERIOD SOLUTIONS

The first family of double lunar swingby orbits are "short period" orbits where the post-LGrA1 (lunar gravity assist 1) orbit period is approximately 14-20 days. These solutions are analogous to the AMC-14 trajectory described above. At the first post-LGrA1 perigee, the spacecraft performs a swingby phasing maneuver (SPM) to target LGrA2. The SPM is an energy management maneuver with thrust along the negative velocity direction. After the SPM, the spacecraft completes one or more revolutions in the phasing orbit before LGrA2. At the first post-LGrA2 perigee, the spacecraft begins a sequence of period reduction maneuver (PRM) to insert into the GEO graveyard.

Targeting Configuration

The short-period solutions use a pair of nested differential correctors for targeting. The inner differential corrector varies the VNC components of the MCC maneuver to achieve a desired target point on the lunar B-plane[8] at LGrA1. B-plane targets are interchangeably formulated either as

Cartesian coordinates ($\vec{B} \cdot \hat{R}$, $\vec{B} \cdot \hat{T}$) or a magnitude-direction pair ($|\vec{B}|$, B_θ). Table 2 summarizes this differential corrector configuration.

Table 2. Inner differential corrector configuration

Controls	Constraints
MCC ΔV_X^{VNC}	$\vec{B} \cdot \hat{R}$ or $\|\vec{B}\|$ at LGrA1
MCC ΔV_Y^{VNC}	$\vec{B} \cdot \hat{T}$ or B_θ at LGrA1
MCC ΔV_Z^{VNC}	

The outer differential corrector varies the LGrA1 B-plane targets as well as the SPM magnitude. The solution is successively refined over three iterations with slightly different targeting parameters. The first run seeks to make the orbit equatorial at the first post-LGrA2 perigee. To avoid constraining RAAN while driving inclination to 0°, the target sequence evaluates the components of the orbit normal vector in the Earth TOD frame. When the X and Y components of the orbit normal are 0, the orbit is equatorial. The second run adds a radius of perigee constraint. The third and final run evaluates the orbit plane and radius of perigee constraints at the end of the orbit lowering phase rather than the first post-LGrA2 perigee. Table 3 shows the outer differential corrector configuration. For each iteration, the header indicates where in the orbit the constraints are evaluated.

Table 3. Outer differential corrector configuration for three successive iterations

Controls	Constraints		
Iteration:	*1*	*2*	*3*
Evaluation:	*Post-LGrA2 perigee*	*Post-LGrA2 perigee*	*Post-PRMs*
SPM ΔV_X^{VNC}	$\hat{n}_X^{TOD}$	$\hat{n}_X^{TOD}$	$\hat{n}_X^{TOD}$
$\vec{B} \cdot \hat{R}$ or $\|\vec{B}\|$ at LGrA1	$\hat{n}_Y^{TOD}$	$\hat{n}_Y^{TOD}$	$\hat{n}_Y^{TOD}$
$\vec{B} \cdot \hat{T}$ or B_θ at LGrA1		$\|\vec{r}\|$	$\|\vec{r}\|$

For the final launch opportunity in the May launch period, it was not possible to converge the trajectory using ballistic lunar swingbys. For the 15-May launch date only, a return powered fly-by (RPF) maneuver was added to LGrA2. This maneuver had thrust constrained along the velocity direction and was included as a control for the final two iterations of the outer differential corrector.

Reference Trajectories

There are three launch opportunities in both the April and May launch period. Figure 4 shows three views of the short-period double lunar swingby orbits with an April launch in the Earth inertial, Earth-Moon rotating-pulsating, and Earth-Sun rotating-pulsating frame. Tick marks are placed every 24 hours. A key distinction of the April-launched short-period orbits is the super-lunar apogee after LGrA1, clearly shown in the inertial and Earth-Sun rotating frames.

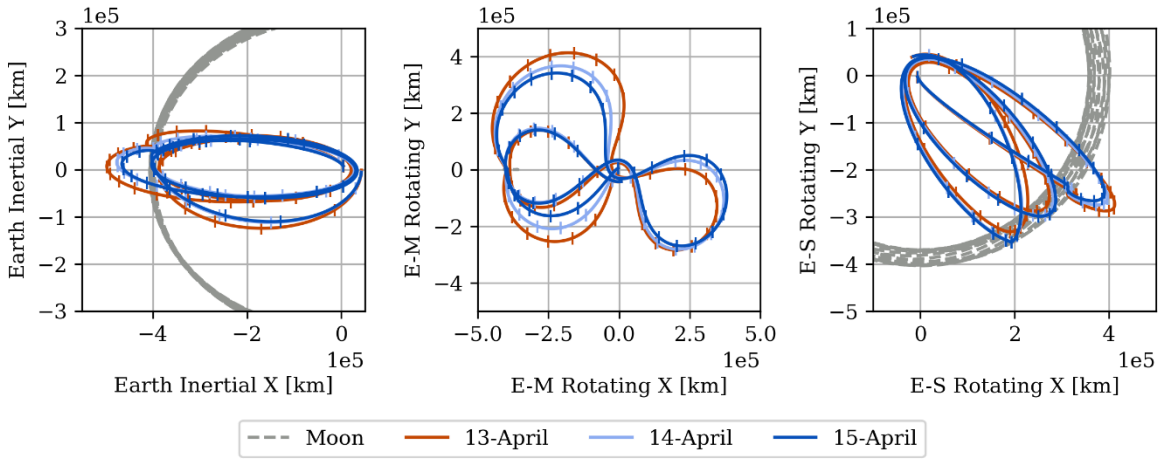

Figure 4. Short period double lunar swingby trajectory for April launch shown in Earth inertial (left), Earth-Moon rotating pulsating (center), and Earth-Sun rotating pulsating (right) frames

The lunar encounter geometry is quite different between LGrA1 and LGrA2. LGrA1 occurs at an altitude between ~5,000-10,000 km while LGrA2 is more distant at ~30,000 km. Figure 5 shows the lunar encounter geometry in the Moon True-of-Date (TOD) frame. The black circle is scaled to mean lunar radius. Since LGrA2 is nearly a polar swingby, the right panel shows the Moon TOD Y-Z plane as opposed to the Moon TOD X-Y plane shown on the left.

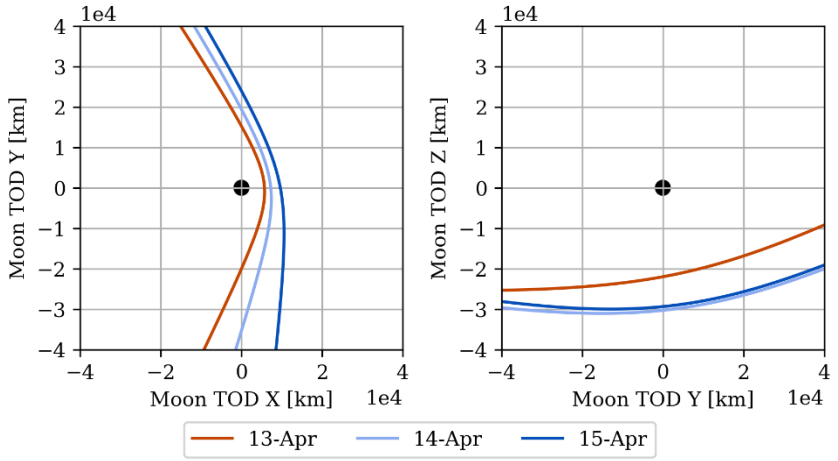

Figure 5. Short period LGrA1 (left) and LGrA2 (right) lunar encounters for April launch shown in Moon TOD frame

The short period orbits with a May launch return directly to perigee after LGrA1 and, as a result, have one less apogee in the phasing orbit. Figure 6 shows three views of the May-launch short period orbits with tick marks every 24 hours. The “missing” apogee is apparent when comparing the middle panel of Figure 6 with the middle panel of Figure 4.

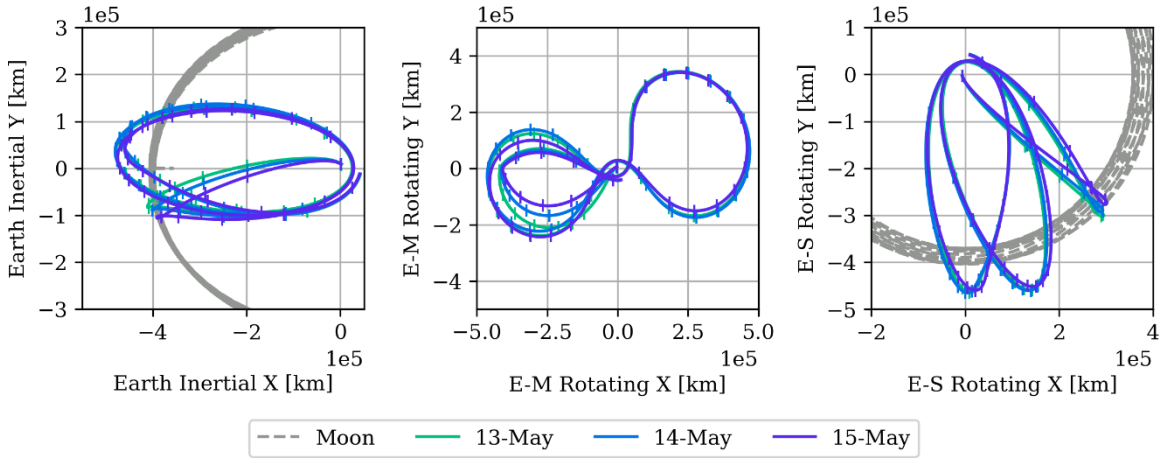

Figure 6. Short period double lunar swingby trajectory for May launch shown in Earth inertial (left), Earth-Moon rotating pulsating (center), and Earth-Sun rotating pulsating (right) frames

The lunar encounter geometry for short period orbits with a May launch is similar to the April launch orbits. LGrA1 remains between ~5,000-10,000 km while LGrA2 is more distant at ~40,000-60,000 km. Figure 7 shows the lunar encounter in the Moon TOD frame. As before, the right panel shows the Y-Z plane while the left panel shows the X-Y plane. LGrA2 for the May-launched orbits is still polar, but to a lesser degree than the for the April-launched orbits.

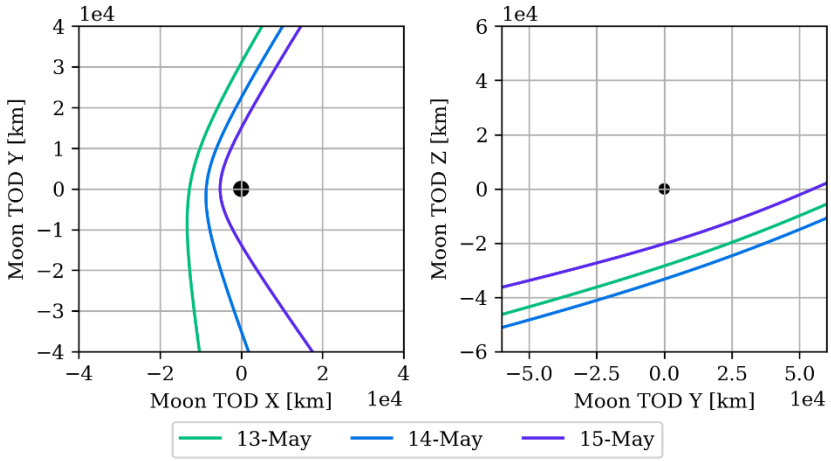

Figure 7. Short period LGrA1 (left) and LGrA2 (right) lunar encounters for May launch shown in Moon TOD frame

Figure 8 shows the altitude profile for both sets of short period double lunar swingby orbits. Altitude is computed to a mean Earth sphere with a radius of 6378.135 km. The altitude profiles clearly show the difference between the April and May launch opportunities. The April-launched orbits continue to apogee after LGrA1 (approximately L+7 days) whereas the May-launched orbits return directly to perigee after LGrA1 (approximately L+5 days).

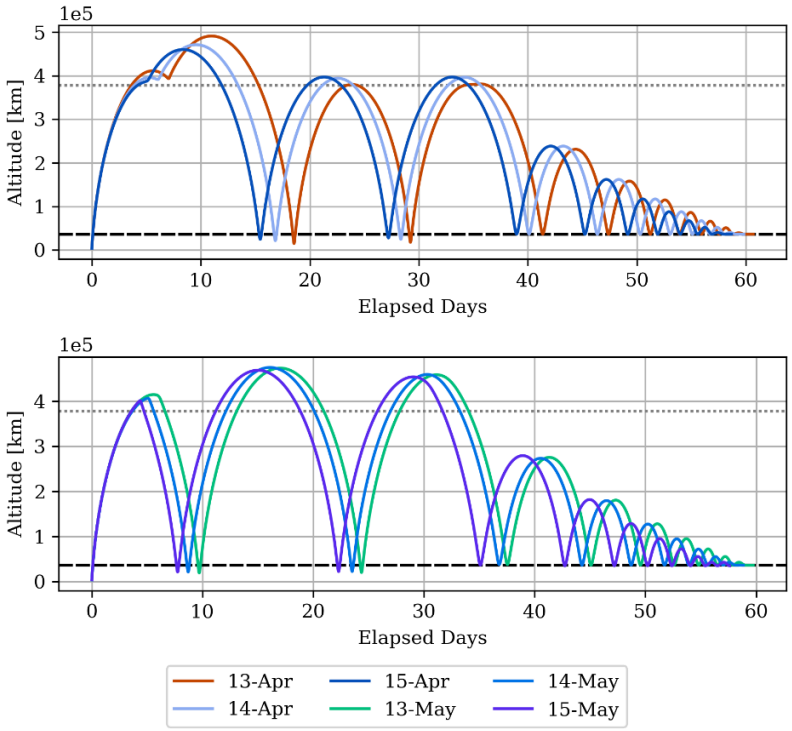

Figure 8. Altitude above Earth mean sphere for short period trajectories after launch in April (top) and May (bottom)

Figure 8 indicates that both perigees in the phasing orbit occur below the GEO belt (shown by the black dashed line). In all six cases, this places the SPM within the Outer Van Allen Belt. This additional passage through the Van Allen Belt increases the total radiation exposure for the spacecraft. The need to perform a maneuver in this regime could also preclude some common radiation mitigation approaches (e.g. minimize spacecraft activity, power off sensitive systems). Additionally, sub-GEO perigees increase the complexity of conjunction analysis and create potential interference with active GEO satellites. To mitigate these concerns, the team sought a set of solutions that did not require a perigee maneuver below GEO.

LONG-PERIOD SOLUTIONS

The second family of double lunar swingby orbits are "long-period" orbits where the post-LGrA1 orbit has a period of approximately 50-80 days. The long-period orbits complete less than one revolution in the phasing orbit and approach the vicinity of the Sun-Earth L2 libration point. The SPM is relocated from perigee (in the short-period orbits) to this high-altitude apogee. Taking advantage of the altitude, a relatively small SPM can target the required LGrA2 geometry. All three components of the SPM can be varied to achieve the LGrA2 targets.

Targeting Configuration

Like the short-period orbits, the long-period orbits use a pair of nested differential correctors. The inner differential corrector is identical to the short-period inner targets and varies the VNC components of the MCC to achieve LGrA1 B-plane targets. Table 2 describes the configuration of this inner differential corrector. The outer differential corrector was configured slightly differently for each trajectory in the long-period family but follows similar logic to that described in Table 3 for the short period orbits. The first two or three iterations are a coarse targeting algorithm to ensure

the trajectory returns to the vicinity of the Moon after apogee. For these coarse differential correctors, fewer controls are used (e.g. only LGrA1 B-plane targets) to ensure the problem is not under-constrained. After generating an initial guess, successive profiles target the final orbit state using a combination of LGrA1 B-plane targets and SPM VNC components. Given three constraints ($\hat{n}_X^{TOD}$, $\hat{n}_Y^{TOD}$, $|\vec{r}|$), differential correctors were generally limited to three controls, chosen from the five available. The trajectory designer selects which controls to use based on feedback from the differential correctors.

Reference Trajectories

Figure 9 shows the long-period double lunar swingby orbits for April launch opportunities in the Earth inertial, Earth-Moon rotating-pulsating, and Earth-Sun rotating-pulsating frame. Given the much longer orbit period, tick marks are placed every 120 hours (5 days). Comparing these trajectories to the short-period orbits, the significantly larger semi-major axis of the phasing orbit is apparent. The Earth-Sun rotating frame clearly shows the apogee approaching the vicinity of Sun-Earth L2 (~1.5e6 km).

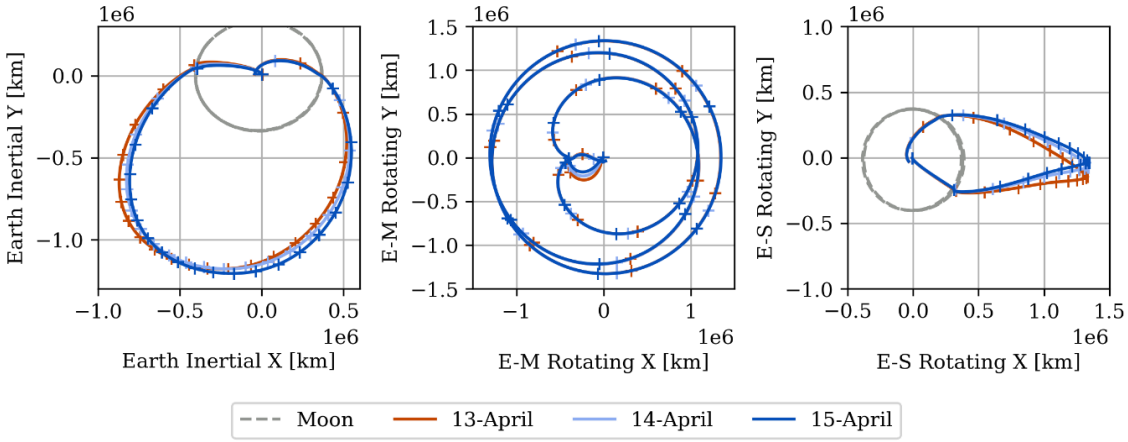

Figure 9. Long period double lunar swingby trajectory for April launch shown in Earth inertial (left), Earth-Moon rotating pulsating (center), and Earth-Sun rotating pulsating (right) frames

For the long-period orbits with an April launch, LGrA1 is a close fly-by at an altitude below 5,000 km. LGrA2 is more distant, occurring between 10,000-20,000 km. Figure 10Figure 5 shows the lunar encounter geometry in the Moon True-of-Date (TOD) X-Y plane. The black circle is scaled to mean lunar radius.

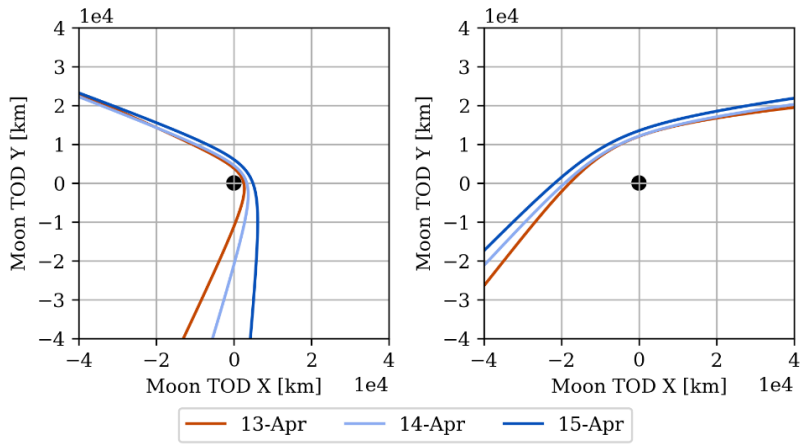

Figure 10. Long period LGrA1 (left) and LGrA2 (right) lunar encounters for April launch shown in Moon TOD frame

Figure 11 shows three views of the long-period double lunar swingby orbits for May launch opportunities with tick marks every 120 hours (5 days). The May-launched orbits have shorter phasing orbits and do not pass as close to Sun-Earth L2 as the April-launched orbits.

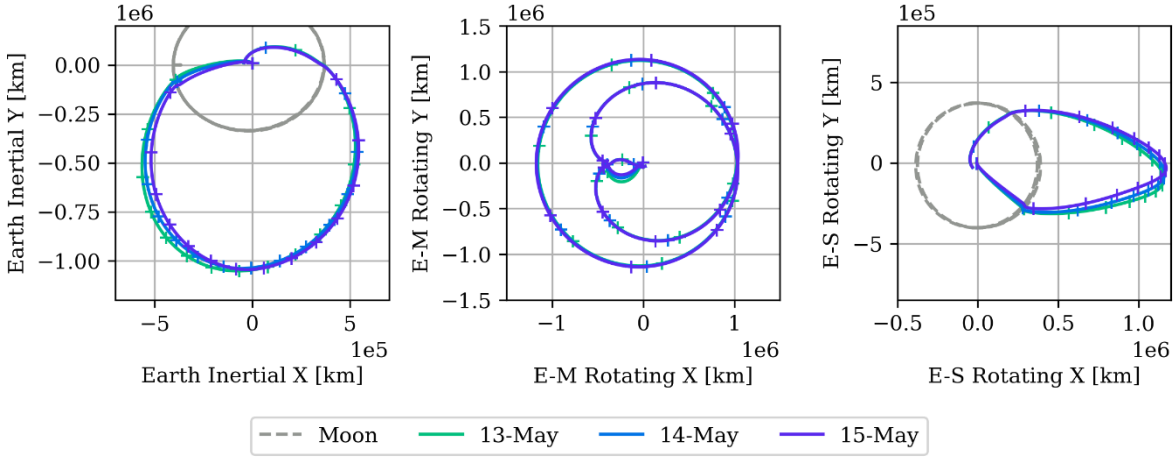

Figure 11. Long period double lunar swingby trajectories for May launch shown in Earth inertial (left), Earth-Moon rotating pulsating (center), and Earth-Sun rotating pulsating (right) frames

Figure 12 shows the lunar encounters for May-launched long-period LGrA1 and LGrA2. The fly-by geometry for the May launch opportunities is very similar to the April geometry.

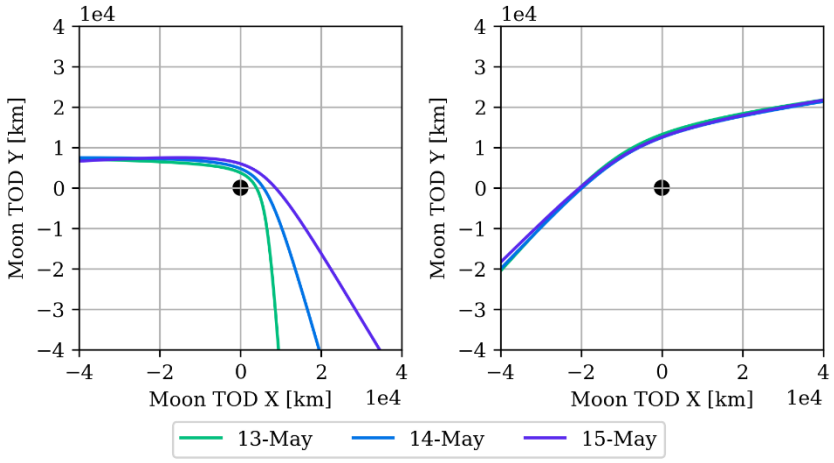

Figure 12. Long period LGrA1 (left) and LGrA2 (right) lunar encounters for April launch shown in Moon TOD frame

Figure 13 shows the altitude profile for both sets of long period double lunar swingby orbits. Altitude is computed to a mean Earth sphere with a radius of 6378.135 km. In Figure 13, the initial epoch for both upper and lower panels is the same (unlike other altitude plots in this work, which reference the initial epoch to the launch or injection time for each trajectory, as applicable). This shows that both sets of long-period orbits target the same lunar encounter for LGrA2. The April launch orbits reach LGrA2 after ~105 days while the May launch orbits require only ~75 days.

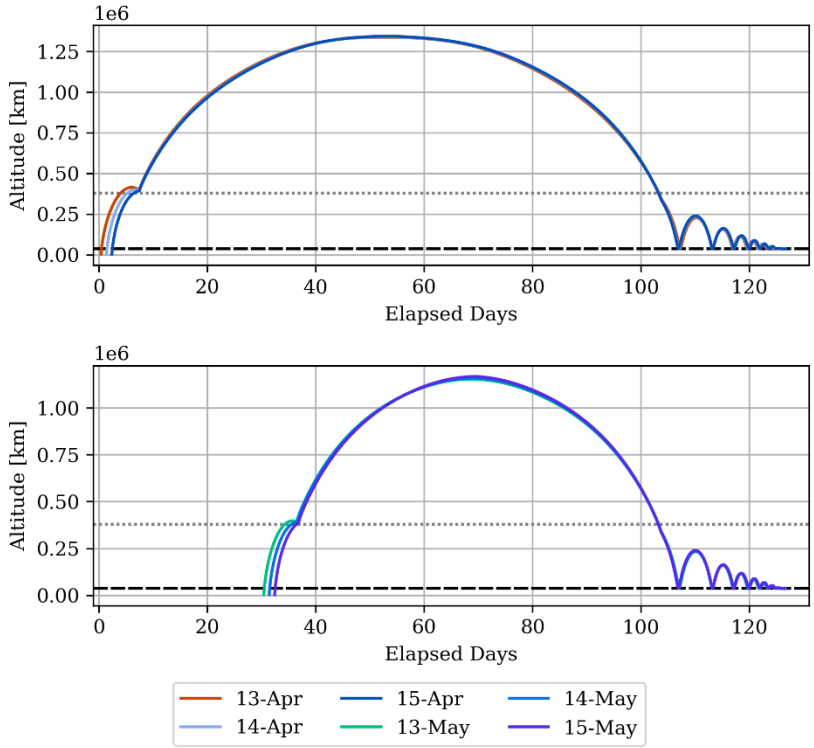

Figure 13. Altitude above Earth mean sphere for short period trajectories after launch in April (top) and May (bottom)

Both sets of long-period orbits remain below 1.5M km and perform all inbound maneuvers above the GEO belt. These positive attributes come at the cost of an increased time-of-flight.

COMPARISON TO SINGLE SWINGBY SOLUTIONS

The short- and long-period families of double lunar swingby orbits demonstrate that two lunar gravity assists can be used to transfer from a lunar rideshare launch to GEO graveyard. Overall, the double lunar swingby orbits satisfy the mission requirements at the expense of additional complexity. Use of these orbits is motivated by the rideshare launch not injecting the spacecraft on a trajectory that encounters the Moon approximately 2° below the equatorial plane. Figure 14 shows the angle to the equatorial plane at the lunar swingby for a representative set of single lunar swingby orbits. Should this condition not be met, a single-swingby orbit is not feasible.

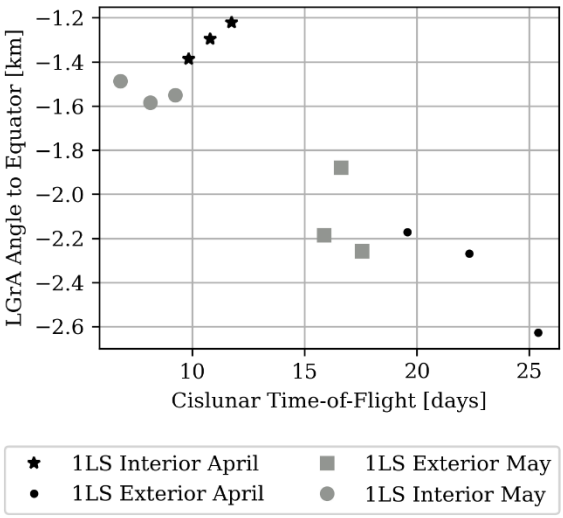

Figure 14. Angle between spacecraft and equatorial plane at LGrA for single lunar swingby (1LS) orbits

To evaluate the relative merit of the double lunar swingby (2LS) orbits as compared to the single lunar swingby (1LS) orbits, we generate a set of 1LS orbits launching in the same April and May periods.

Single Swingby Reference Solutions

The simplest 1LS trajectory requires no deterministic maneuvers and directly targets the required LGrA from launch. Since the representative rideshare injection states do not encounter the Moon at the required point in its orbit, the 1LS reference solutions assume a targeted launch. This assumption is not applicable to rideshare missions but does generate the most optimistic 1LS orbits for comparison purposes. Policastri et al describe the process for designing 1LS orbits originating from a rideshare launch and identify two families of 1LS orbits: exterior and interior.[1] The exterior family has a post-LGrA apogee while the interior family proceeds directly to perigee. In this aspect, the exterior and interior 1LS families are comparable to the April and May short-period 2LS families.

To target 1LS orbits from a dedicated launch, a single differential corrector is used with multiple profiles to successively refine the trajectory to achieve the desired final orbit state. The initial state for these reference trajectories results from a simple launch-coast-burn model. Cape Canaveral is assumed to be the launch site and the parking orbit inclination is set to 28.5°. An initial guess for

the 1LS orbit is generated by first determining a trans-lunar injection (TLI) burn magnitude and parking orbit coast period that place apogee near the Moon. Next, launch epoch, coast duration, and TLI magnitude are varied first to hit a manually selected LGrA B-plane target and finally to achieve the required orbit plane and perigee radius.

Figure 15 and Figure 16 show three views of the exterior and interior 1LS orbits, respectively for both the April and May launch periods. The exterior orbits have a super-lunar apogee after the LGrA whereas the interior orbits proceed directly to perigee.

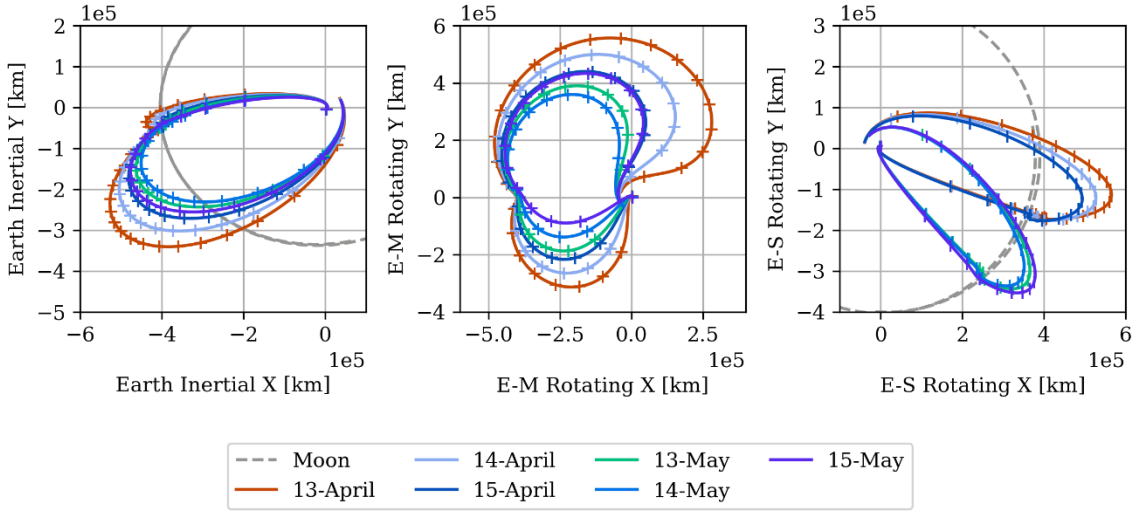

Figure 15. Exterior single lunar swingby trajectories shown in Earth inertial (left), Earth-Moon rotating pulsating (center), and Earth-Sun rotating pulsating (right) frames

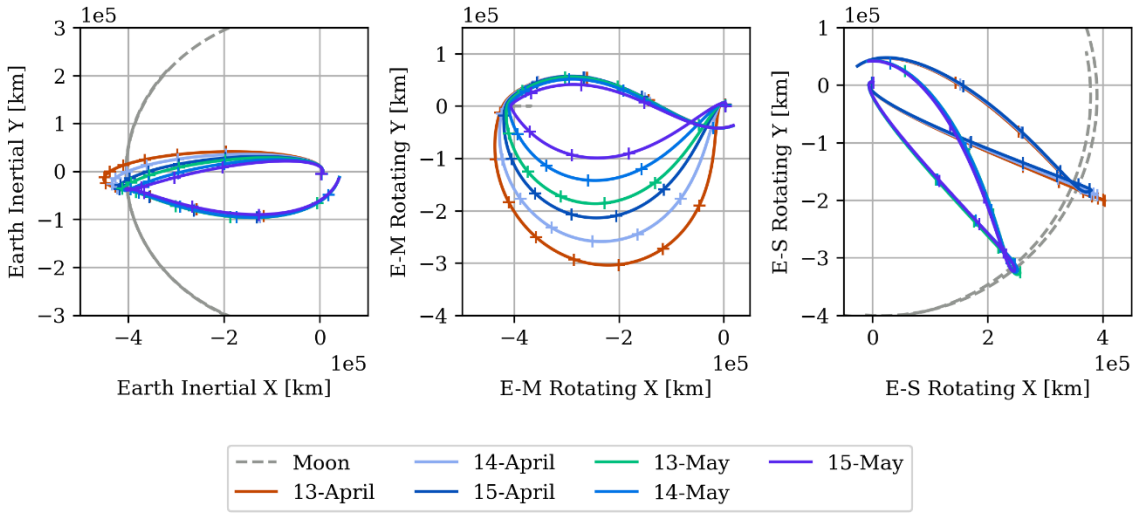

Figure 16. Interior single lunar swingby trajectories shown in Earth inertial (left), Earth-Moon rotating pulsating (center), and Earth-Sun rotating pulsating (right) frames

Figure 17 shows the LGrA geometry for both exterior and interior orbits. As compared to the 2LS orbit, the 1LS LGrA span a much wider range of altitudes, from <1,000-20,000 km. Figure 18 shows the altitude profile for the exterior and interior 1LS orbits. The black dashed line indicates

GEO graveyard altitude while the grey dotted line shows the approximate lunar orbit distance, for reference.

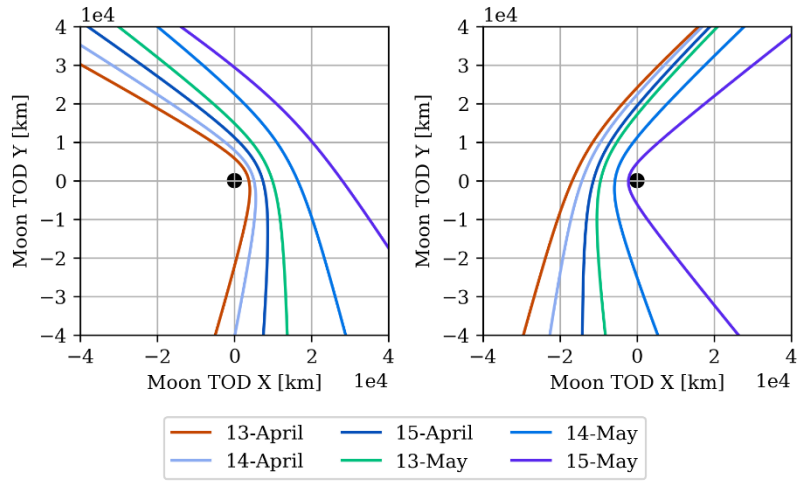

Figure 17. Exterior (left) and interior (right) lunar encounters for single lunar swingby trajectories shown in Moon TOD frame

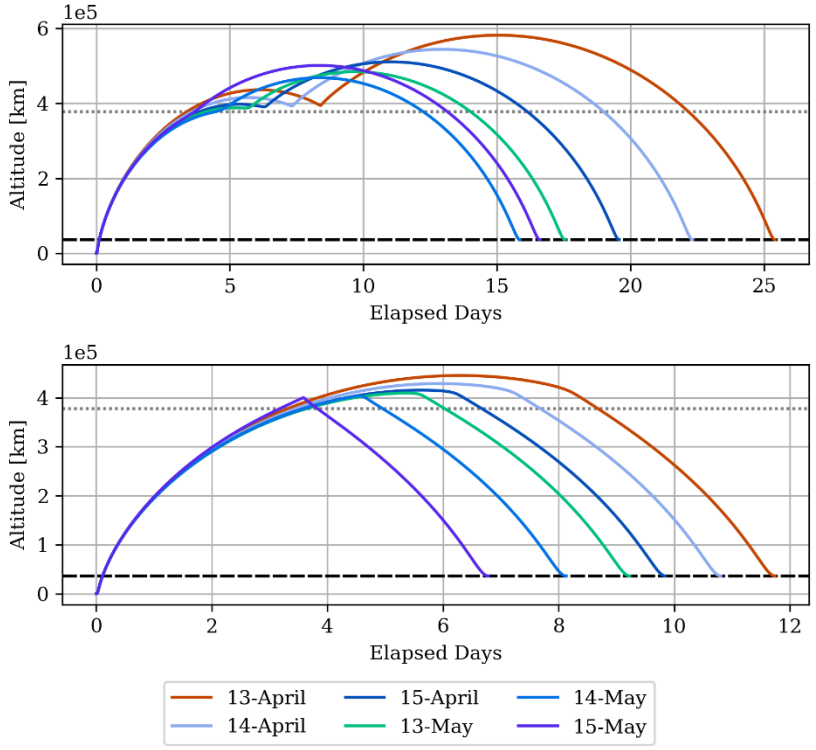

Figure 18. Altitude above Earth mean sphere for exterior (top) and interior (bottom) single lunar swingby trajectories

Summary Results

Figure 19 compares the LGrA1 and LGrA2 altitudes for the 1LS and 2LS orbits. The 1LS orbits, by definition, only have a single fly-by that is shown with LGrA1 for the 2LS orbits.

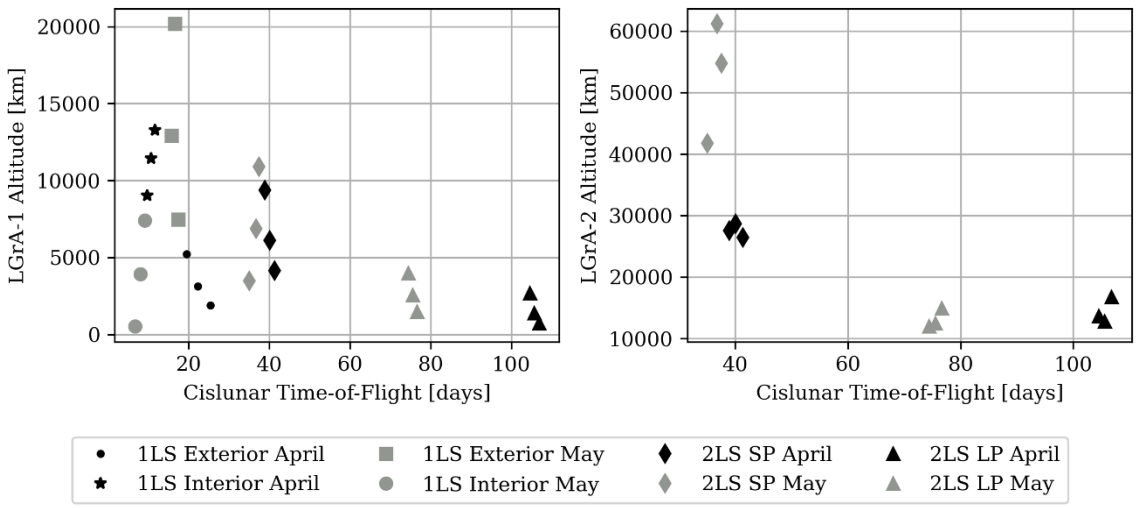

Figure 19. LGrA1 (left) and LGrA2 (right) altitudes for 1LS and 2LS orbit families

All comparison plots use the cislunar time-of-flight, defined as the duration from launch (or separation) to the first perigee at GEO radius, as the horizontal axis. For both the 1LS and 2LS orbits, the orbit lowering (PRM) phase is a nearly constant duration and can be neglected for comparison purposes. The horizontal axis shows the significantly longer duration, ~90-130 days, of the 2LS long-period orbits. The 1LS orbits have the shortest cislunar time-of-flight from ~10-30 days. For LGrA1, the 1LS orbits launched in May exhibit a much greater range of swingby altitudes than the 2LS orbits. For all orbits, LGrA1 is below ~20,000 km.

Figure 20 shows the required ΔV during the cislunar phase and for the entire trajectory (including orbit lowering). Since the 1LS trajectories are ballistic and targeted from launch, they require no cislunar ΔV. The 1LS data points shown on the right panel represent the ΔV required for orbit lowering only.

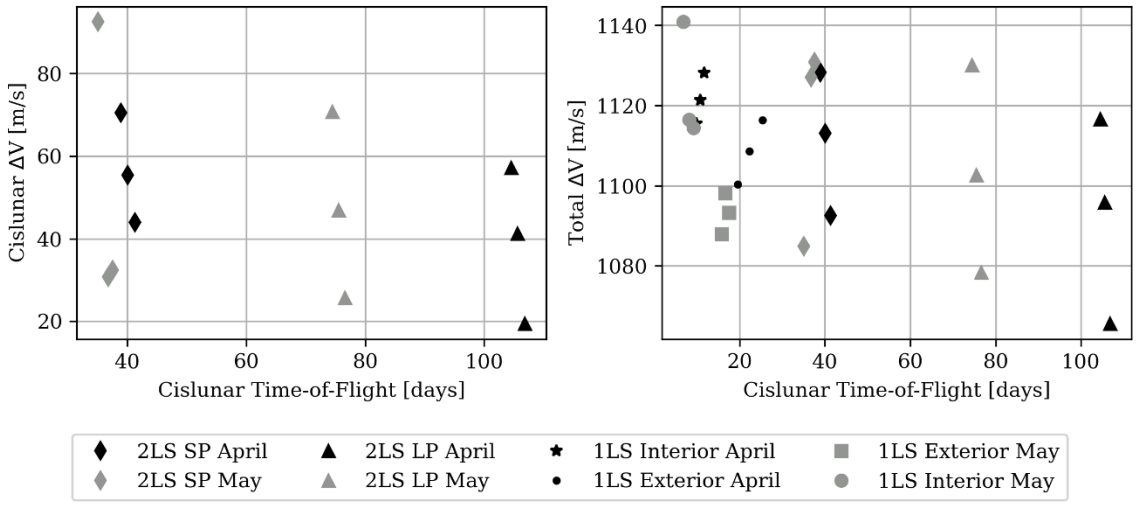

Figure 20. Cislunar (left) and total (right) ΔV required for 1LS and 2LS orbit families

Figure 20 demonstrates that the majority of ΔV required for any lunar swingby to GEO trajectory comes from the orbit lowering rather than the cislunar phase. All trajectories require >1 km/s

ΔV to reduce semi-major axis and insert into GEO graveyard. This reality stems from the required apogee altitude to set up the lunar encounter. The ΔV to reach lunar distance is provided by the launch vehicle but the spacecraft must have sufficient ΔV to reduce energy down to GEO. Variation in the orbit lowering ΔV is caused by varying post-LGrA1 semi-major axes. The additional ΔV required for cislunar phase maneuvers ranges from ~20-90 m/s across all 2LS orbits. On average, the short-period orbits require more ΔV than the long-period.

Finally, Figure 21 shows the maximum and minimum altitudes for both 1LS and 2LS orbit families. The minimum altitude is computed after 5 days to eliminate the outgoing leg of both trajectory families.

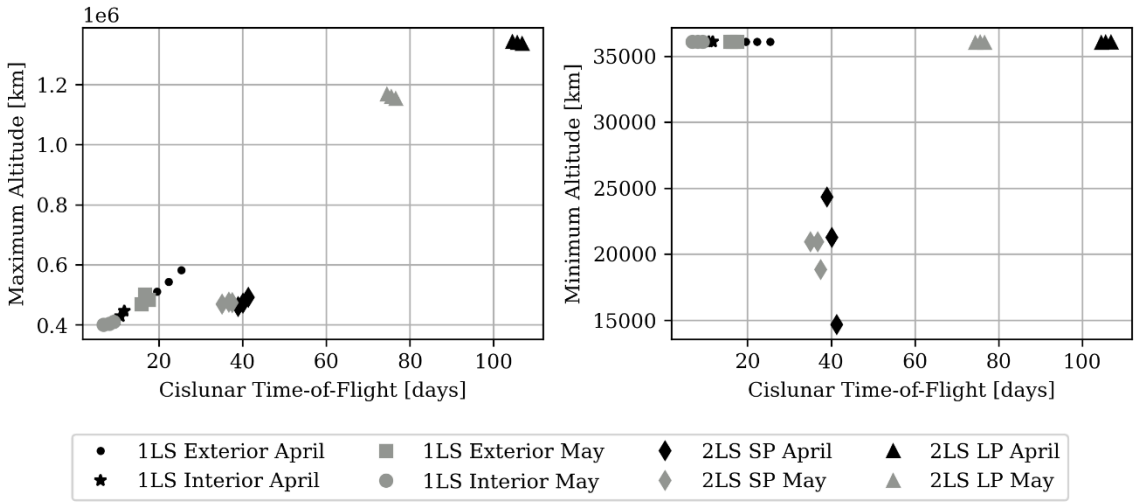

Figure 21. Maximum (left) and minimum (right) altitudes for 1LS and 2LS orbit families

As expected, the long-period 2LS orbits have by far the greatest maximum altitude. The short-period 2LS orbits are enveloped by the range of 1LS orbits maximum altitude. This illustrates the key difference in terms of communication link requirements between the short- and long-period 2LS orbits. Pivoting from a 1LS or short-period 2LS orbit to the long-period 2LS orbit imposes the requirement to communicate at approximately double the range (~1.2M km vs. ~600,000 km).

The altitude range for 1LS and long-period 2LS orbits is the GEO graveyard altitude. This indicates that neither of these trajectory families pass below the GEO belt after the outbound leg (launch to LGrA1). The short-period 2LS orbits have minimum altitudes between ~15,000-25,000 km, below GEO and the approximate upper limit of the outer Van Allen Belts. This undesirable feature counterbalances the shorter time-of-flight of the short-period orbits.

DISCUSSION

The existence of short- and long-period double lunar swingby orbits that meet mission requirements demonstrates that this class of trajectory is an option for GEO payloads launched as rideshares with lunar missions. Between the scarcity of GTO launches and the increasing frequency of lunar payload launches, operators may find lunar rideshare a more viable option for delivering secondary payloads to GEO or near-GEO. In that case, the ability to mitigate sub-optimal lunar encounter geometry becomes critical. The requirements and constraints driving lunar orbiter or lunar lander launch targeting are dissimilar from those driving a swingby-to-GEO mission. Multi-gravity-assist trajectories that deliver the payload to the same final orbit state increase compatibility

with rideshare opportunities and reduce the likelihood of changes in the primary payload's launch targets interfering with the secondary payload's trajectory.

Between the short- and long-period double lunar swingby orbits, the short-period orbits are attractive for their short time-of-flight and lower maximum altitude. Unfortunately, the short-period orbits for April and May launch opportunities have multiple perigees below GEO and within the Van Allen Belts. Furthermore, a maneuver is required in this region, precluding some common radiation mitigation options. Should potential GEO interference or increased radiation exposure not be a concern for a given spacecraft or payload, the short-period orbits may be a viable option.

The long-period double lunar swingby orbits eliminate the perigee maneuver by using LGrA1 to increase apogee and performing the SPM at this high-altitude apogee. While avoiding the Van Allen Belts and potential GEO conflicts, the long-period orbits do require communication in the vicinity of Sun-Earth L2 and a significantly longer time of operation in deep space.

As expected, all double lunar swingby orbits exhibit longer time-of-flight than single swingby orbits. In general, missions sensitive to time-of-flight would select the single double swingby over the double swingby orbits. However, for rideshare missions manifested with a given primary payload, the double lunar swingby orbits may enable successful transfers to GEO where a single lunar swingby cannot.

CONCLUSION

SEE developed double lunar swingby trajectories from a lunar rideshare launch to the GEO graveyard. Both short-period and long-period solutions exist, offering a trade-off between maneuver complexity, time-of-flight, and maximum spacecraft-to-Earth range. The required ΔV for these solutions compares favorably with idealized single lunar swingby trajectories. Double lunar swingby orbits create opportunities for GEO missions to rideshare with lunar payloads. Further development of these trajectories will require evaluating the sensitivity of both LGrAs to navigation and maneuver execution errors. From these results, the magnitude of statistical trajectory correction maneuvers (TCMs), unmodeled in this analysis, can be estimated.

ACKNOWLEDGEMENTS

The authors thank SEE colleagues Marissa Intelisano and Lisa Policastri for their insightful questions, comments, and discussion about the mission requirements, concept of operations, and navigation considerations for these trajectories.

REFERENCES

[1] L. Policastri, M. Intelisano, M. Loucks, and S. West, “Mission design for the Sherpa GEO Pathfinder.” AAS/AIAA Astrodynamics Specialist Conference, Charlotte, NC, 2022.

[2] R. Battin and J. Miller, “Circumlunar trajectory calculations.” MIT Instrumentation Laboratory Report R-353, 1962.

[3] D.W. Dunham and S.A. Davis, “Catalog of double lunar swingby orbits for exploring the Earth’s geomagnetic tail.” NASA CR-160066, 1980.

[4] J. Carrico, H.L. Hooper, L. Roszman, and C. Gramling, “Rapid design of gravity assist trajectories.” 3rd International Symposium on Spacecraft Flight Dynamics, Darmstadt, Germany, 1991.

[5] C. Ocampo, “Trajectory Analysis for the Lunar Flyby Rescue of AsiaSat-3/HGS-1.” Ann. N.Y. Acad. Sci. 1065:232-253, 2005.

[6] Inter-Agency Space Debris Coordination Committee, “IADC Space Debris Mitigation Guidelines.” IADC-02-01 Rev. 3, 2021.

[7] Short, C, et al, “Revisiting Trajectory Design with STK Astrogator, Part 2”, AAS 21-561, AAS/AIAA Astrodynamics Specialist Conference, Big Sky, Montana, USA, August 2021.

[8] D. Farnocchia, S. Eggl, P.W. Chodas, J.D. Giorgini, and S.R. Chesley, “Planetary encounter analysis on the B-plane: a comprehensive formulation.” Celestial Mechanics and Dynamical Astronomy 131:36, 2019.